APL Materials

Variable temperature probing of minority carrier transport and optical properties in *p*-Ga_2O_3

Cite as: APL Mater. **10**, 031106 (2022); https://doi.org/10.1063/5.0086449
Submitted: 25 January 2022 • Accepted: 21 February 2022 • Published Online: 08 March 2022

Sushrut Modak, Leonid Chernyak, Alfons Schulte, et al.

Variable temperature probing of minority carrier transport and optical properties in p-Ga_2O_3

Cite as: APL Mater. 10, 031106 (2022); doi: 10.1063/5.0086449
Submitted: 25 January 2022 • Accepted: 21 February 2022 •
Published Online: 8 March 2022

Sushrut Modak[1] Leonid Chernyak,[1,a)] Alfons Schulte,[1] Corinne Sartel,[2] Vincent Sallet,[2] Yves Dumont,[2] Ekaterine Chikoidze,[2] Xinyi Xia,[3] Fan Ren,[3] Stephen J. Pearton,[4] Arie Ruzin,[5] Denis M. Zhigunov[6] Sergey S. Kosolobov,[6] and Vladimir P. Drachev[6]

AFFILIATIONS

[1] Department of Physics, University of Central Florida, Orlando, Florida 32816, USA
[2] Groupe d'Etude de la Matière Condensée, Université Paris-Saclay, Université de Versailles Saint Quentin en Yvelines–CNRS, 45 Av. des Etats-Unis, 78035 Versailles Cedex, France
[3] Department of Chemical Engineering, University of Florida, Gainesville, Florida 32611, USA
[4] Material Science and Engineering, University of Florida, Gainesville, Florida 32611, USA
[5] School of Electrical Engineering, Tel Aviv University, Tel Aviv 69978, Israel
[6] Center for Engineering Physics, Skolkovo Institute Science and Technology, Nobel St., Bldg. 1, Moscow 121205, Russia

[a)] **Author to whom correspondence should be addressed:** chernyak@physics.ucf.edu

ABSTRACT

Electron beam-induced current in the temperature range from 304 to 404 K was employed to measure the minority carrier diffusion length in metal–organic chemical vapor deposition-grown p-Ga_2O_3 thin films with two different concentrations of majority carriers. The diffusion length of electrons exhibited a decrease with increasing temperature. In addition, the cathodoluminescence emission spectrum identified optical signatures of the acceptor levels associated with the V_{Ga}^{-}–V_O^{++} complex. The activation energies for the diffusion length decrease and quenching of cathodoluminescence emission with increasing temperature were ascribed to the thermal de-trapping of electrons from V_{Ga}^{-}–V_O^{++} defect complexes.

β-Ga_2O_3 is an emerging fourth-generation power electronics platform with a wide-bandgap of ~4.8 eV and a high breakdown field (8×10^6 V cm^{-1}).[1–6] It is becoming increasingly attractive due to its applications in high-power electronics, true solar-blind UV detection, and optoelectronic devices.[2,3,7–10] Undoped β-Ga_2O_3 tends to be n-type due to unintentional donor impurities such as Si. Intentionally, n-type β-Ga_2O_3 can be obtained by adding controlled amounts of impurities such as Si, Sn, and Ge, which is well documented.[3,5] Carrier transport characterization revealed impurity bands and the hopping mechanism of electrical transport in such doped films.[11–14] Low-temperature electron mobilities up to 796 cm^2/V s[13] have been reported. The incorporation of doped layers in devices such as Schottky diodes and field-effect transistors (FETs), including metal–oxide–semiconductor FETs (MOSFETs), and their ability to withstand high energy particle radiation have been explored.[15–24] Replicating these results to achieve p-type conductivity in β-Ga_2O_3 has proven very difficult due to factors such as doping asymmetry, high compensation of acceptors, the high ionization energy of acceptor levels, and hole-trapping at O(I) and O(II) sites.[25–30] Despite these difficulties, native p-type conductivity was demonstrated at high temperatures in undoped β-Ga_2O_3.[31,32] It was observed that native p-type conductivity is achievable by creating a significant number of native acceptors (V_{Ga}) and suppressing the compensation due to native donors (V_O). The thermodynamic balance required to weaken the self-compensation in undoped β-Ga_2O_3 was achieved by adjusting the growth temperatures and oxygen partial pressures during the deposition of Ga_2O_3 on sapphire substrates by Metal–Organic Chemical Vapor Deposition (MOCVD).[32,33]

p-type β-Ga_2O_3 is a relatively recent discovery and an uncharted territory in terms of minority carrier transport and

luminescence characterization as well as their temperature dependences. Knowledge of minority carrier (electrons) transport properties in p-type β-Ga_2O_3 is essential for achieving bipolar technology on the gallium oxide platform. In this report, the diffusion length of minority carriers (electrons), cathodoluminescence, and their temperature dependence are studied in p-type β-Ga_2O_3 with two different majority carrier (holes) concentrations.

Undoped β-Ga_2O_3 samples, analyzed in this study, were grown in an RF-heated horizontal MOCVD reactor with separate inlets to avoid premature reactions in the manifold between oxygen and organometallics precursors. Trimethylgallium (TMGa) and 5.5 N pure oxygen were used as gallium and oxygen sources, respectively. Argon was used as the carrier gas (cf. Ref. 32). The β-Ga_2O_3 layer was grown on a c-oriented sapphire substrate using Ga/O ratio and growth temperature as 1.4×10^{-4} and 775 °C, respectively. Two different total reactor pressures of 30 and 38 Torr and variable growth rates (gallium and oxygen precursor fluxes) were used to create two different native defect (V_{Ga} and V_O) concentrations in the Ga_2O_3 films, leading to the different values of p-type conductivity. The difference between the total reactor pressures for the deposition of the two samples is due to a change in the oxygen partial pressure. The concentration of native defects responsible for p-type conductivity is sensitive to the oxygen partial pressure. The epitaxial layer thickness was ~450 nm. X-ray diffraction scans revealed highly textured films of gallium oxide in the β-Ga_2O_3 phase with a monoclinic space group ($C2/m$) symmetry. Hereinafter, the sample grown under 30 Torr total reactor pressure will be labeled A and that grown under 38 Torr will be labeled B.

A detailed study of the electrical transport properties for the above-referenced highly resistive (close to stoichiometric) Ga_2O_3 samples has been performed. Ohmic contacts were prepared with silver paint at the four corners of the sample. Hall effect measurements were conducted in a van der Pauw configuration in the 500–850 K temperature range for magnetic fields perpendicular to the film plane varying from −1.6 to 1.6 T using a high impedance high-temperature custom-designed measurement setup. Resistivities at highest measured T = 850 K were found to be ρ (A) = 1.2×10^3 **Ω** cm and ρ (B) = 1.3×10^4 Ω cm. Hall effect measurements demonstrated (cf. Refs. 31 and 32) the positive sign for majority carriers in both samples, thus confirming the p-type conductivity. The free hole concentrations and mobilities at 850 K were estimated as follows: p = 5.6×10^{14} cm^{-3} and μ = 8.0 cm^2 V^{-1} s^{-1} for sample A and p = 2.7×10^{13} cm^{-3} and μ = 16 cm^2 V^{-1} s^{-1} for sample B. Temperature-dependent measurements were possible to perform only down to 520 K (p = 2.0×10^{10} cm^{-3}) for sample A and only to 620 K for sample B (p = 7.1×10^{10} cm^{-3}) due to the samples' high resistivity. The difference in hole concentrations is due to the difference in growth conditions (total reactor pressure and the ratio of gallium–oxygen precursor fluxes), resulting in the variation of electrical compensation degree $K = N_A/N_D$, i.e., the ratio of native acceptor to native donor concentrations. Ni/Au (20/80 nm) asymmetrical pseudo-Schottky contacts were created on the film with lithography/liftoff techniques for further analysis.

Electron Beam-Induced Current (EBIC) and cathodoluminescence (CL) measurements were performed *in situ* in a Phillips XL-30 Scanning Electron Microscope (SEM) to characterize the diffusion length (L) of minority carriers (electrons) and luminescence

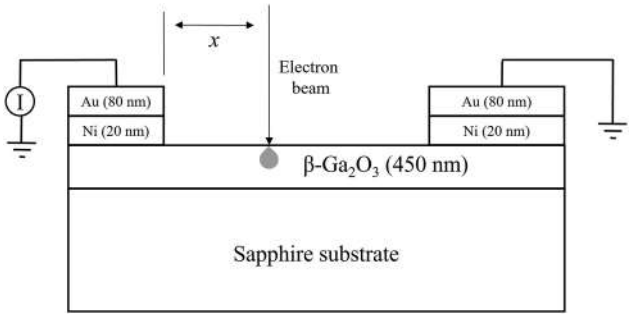

FIG. 1. A schematic diagram of the sample structure and experimental setup.

behavior of the samples, respectively. The measurements were carried out in the 304–404 K temperature range using a Gatan MonoCL2 temperature-controlled stage integrated into the SEM. For both EBIC and CL measurements, the electron beam energy was kept at 10 keV. The EBIC line scans were obtained in a planar configuration (Fig. 1). The EBIC signal was amplified with a Stanford Research Systems SR 570 low-noise current amplifier and digitized with a Keithley digital multimeter (DMM) 2000 controlled by a personal computer (PC) using homemade software. CL measurements were carried out using a Gatan MonoCL2 attachment to the SEM. Spectra were recorded with a Hamamatsu photomultiplier tube sensitive in 150–850 nm range and a single grating monochromator (blazed at 1200 lines/mm).

EBIC line-scans were used to extract diffusion length, L, from the following equation:[34,35]

$$C(x) = C_0 x^{\alpha} \exp\left(-\frac{x}{L}\right), \quad (1)$$

where C(x) is the EBIC signal at distance x from the Schottky junction, C_0 is a scaling constant, x is the distance of the electron beam from the Schottky barrier, and α is the linearization parameter, related to surface recombination velocity. The coefficient α was set at −0.5, corresponding to the low influence of surface recombination. Since the carrier concentration is low in both samples, the Schottky barrier depletion width is significantly larger than L and, therefore, the approach outlined in Ref. 36 was used. Figures 2(a) and 2(b) show the raw EBIC signals and a fit with $x^{\alpha} \exp(-x/L)$ used in extracting L for samples A and B, respectively. The temperature dependence of L for samples A and B is shown in Fig. 3. L decreased with increasing temperature, with values for samples A and B at 304 K of 1040 and 8506 nm, respectively. At 404 K, L reduced to 640 and 6193 nm, respectively. Relatively large values of L are partially due to the shallow majority carrier concentration. Within the current temperature range of measurements, the origin of L decrease is likely due to phonon scattering.[37] Reported values of L for minority carrier (holes) in n-type β-Ga_2O_3 are within 50–600 nm,[20,21,38–41] lower than those of electrons measured in this work for minority carrier electrons. A likely reason could be the large effective mass for holes (18–25 m_0).[42] It is worth noting that a similar dependence of L on temperature was found for n-type β-Ga_2O_3, but it is attributed to scattering on ionized impurities due to heavy Si doping.[41] The activation energy for the temperature dependence of L is given by[43,44]

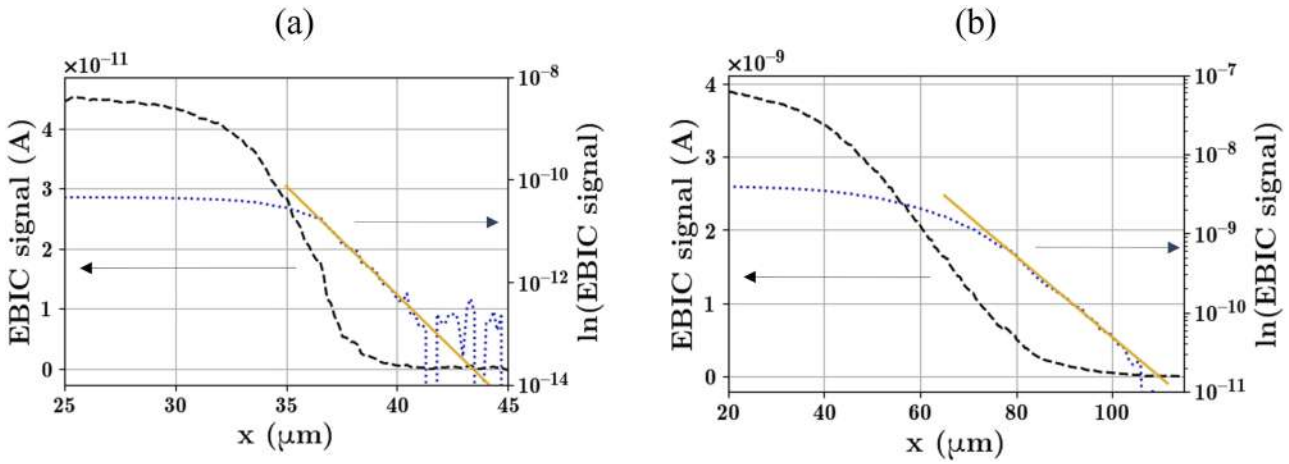

FIG. 2. An example of the acquired EBIC line-scan from sample A (a) and sample B (b) at 304 K along with $\exp(-x/L)/x^{0.5}$ fit for extraction of the diffusion length.

$$L(T) = L_0 \exp\left(\frac{\Delta E_{L,T}}{2kT}\right), \quad (2)$$

where L_0 is a scaling constant, $\Delta E_{L,T}$ is the thermal activation energy, k is the Boltzmann constant, and T is the temperature. The activation energy pertaining to the reduction of L with temperature is 67 and 113 meV for samples A and B, respectively. A detailed discussion regarding the origin of $\Delta E_{L,T}$ is given later in the text.

Raw CL spectra and their Gaussian decompositions at 304 K are presented in Figs. 4(a) and 4(b) for samples A and B, respectively.

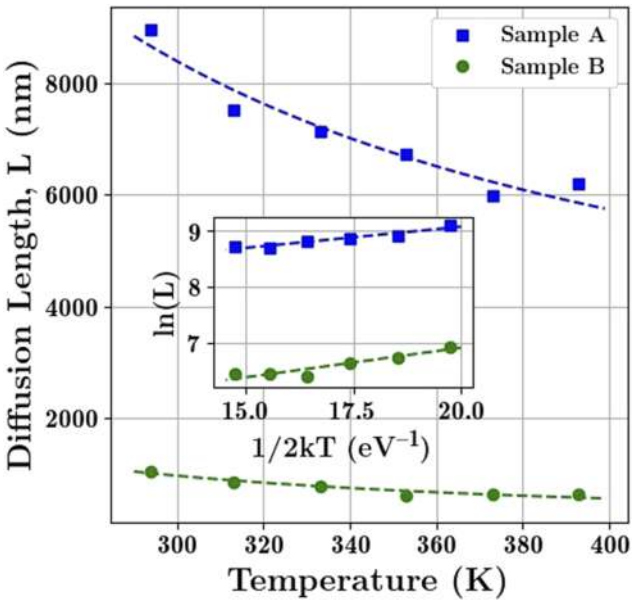

FIG. 3. Temperature dependence of the diffusion length for samples A and B. The inset shows the Arrhenius plot with a linear fit for extraction of the activation energy $\Delta E_{L,T}$.

The CL spectra exhibit four characteristic luminescence bands: ultraviolet (UVL′ and UVL) at 375 and 415 nm, blue (BL) at 450 nm, and green (GL) at 520 nm. The UVL′ and UVL bands are commonly ascribed to recombination of self-trapped excitons, considering the absence of near band edge emission and their lack in β-Ga_2O_3 for sub-bandgap excitation.[26,27,29,45–48] The self-localization of excitons occurs at O(I) and O(II) site, corresponding to UVL′ and UVL bands, respectively.[47,49] Although, as has been shown from Electron Paramagnetic Resonance (EPR) measurements[50] and confirmed by several independent EBIC studies on n-type β-Ga_2O_3,[20–23,39,51,52] the self-localization of holes is unstable above 110 K, the optical signature of the self-trapped excitons persists in CL and photoluminescence (PL) measurements. Note that the relative contribution of UVL′ and UVL bands in both A and B samples is much lower than in n-type β-Ga_2O_3, found in earlier reports.[26,47,49,53–58] The BL band arises from donor–acceptor pair recombination involving a V_O donor and V_{Ga} or a (V_O, V_{Ga}) complex as an acceptor. GL has several different origins, mentioned in the literature, and was observed with an array of various dopants, such as Mg,[59] Si,[54] and Er.[60] In undoped β-Ga_2O_3, grown by floating zone technique, Víllora *et al.*[61] ascribed GL to self-trapped excitons as it existed only for PL excitation energies below the bandgap. Moreover, this band was also observed in β-Ga_2O_3 nanoflakes, structurally consisting of a crystalline core and amorphous shell.[62,63] In a recent study on β-Ga_2O_3 films on a c-plane sapphire substrate with (201) orientation, deposited with magnetron sputtering,[64] the intensities of BL and GL were modulated by changing the oxygen flow rate, and the origin of the GL was attributed to the presence of isolated V_{Ga}. Furthermore, the presence of isolated V_O did not independently play a role in enhancing BL, and the origin of BL was assigned to a defect complex involving V_O and V_{Ga}. Given the abundance of isolated V_{Ga} acceptors and (V_O, V_{Ga}) complexes in both samples, a relatively large contribution of both BL and GL to the CL emission spectrum is observed in this work. Binet and Gourier[53] and Onuma *et al.*[49] independently found a correlation between conductivity and concentration of the V_O donors in n-type β-Ga_2O_3. In this case, since V_O compensates the acceptors, and due to the

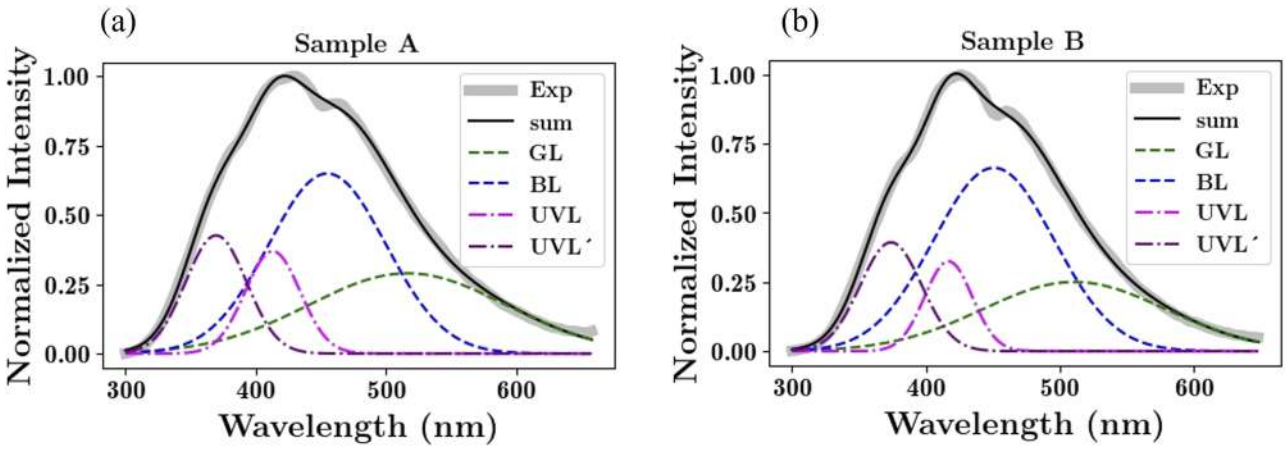

FIG. 4. Normalized CL spectrum for sample A (a) and sample B (b) and their Gaussian decomposition into four bands: UVL′, UVL, BL, and GL.

high ionization energy of acceptors, p-type β-Ga_2O_3 has relatively high resistivity below 450 K.[31,32] The presence of a rather large number of V_{Ga} acceptors and (V_O, V_{Ga}) acceptor complexes, promoting p-type conductivity, was confirmed from the CL emission spectrum.

The temperature dependence of the CL signal follows the form[53]

$$I(T) = I_0/(1 + e^{\Delta E_{CL}/kT}), \tag{3}$$

where I(T) is the integrated CL intensity, I_0 is a constant, and ΔE_{CL} is the process activation energy. Figure 5 shows the Arrhenius plot of $\ln(I_0/I(T) - 1)$. The process activation energy ΔE_{CL}, obtained from a linear fit of the temperature dependence depicted in Fig. 5, was 88 and 101 meV for samples A and B, respectively. The total CL intensity is used in Fig. 5 because the relative contributions of the individual luminescence bands remained approximately constant in the temperature range of the measurements. The activation energies $\Delta E_{L,T}$ and ΔE_{CL} for sample A (67 and 88 meV, respectively) and sample B (113 and 101 meV, respectively) are comparable and can be attributed to a common origin.

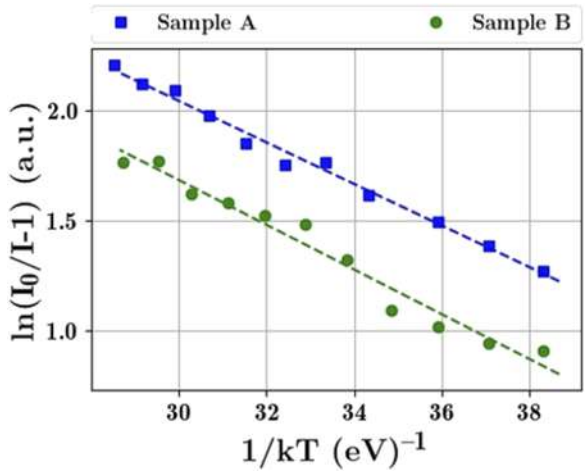

FIG. 5. Arrhenius plot of $\ln(I_0/I(T) - 1)$ vs 1/(kT) from Eq. (1), where I is the integrated CL emission intensity, with the fit, used in the extraction of activation energy (ΔE_{CL}) for the thermal quenching process.

Temperature-dependent resistivity measurements between 300 and 850 K in our earlier study[32] on deep V_{Ga} acceptor defects in similar Ga_2O_3 samples showed two activation energies due to temperature-activated processes. In the high temperature region (T > 400 K), the acceptors are ionized with an activation energy of 0.56 eV. However, for temperatures between 300 and 400 K, a shallower V_{Ga}^{-}–V_O^{++} acceptor complex is present. The concentration of this complex strongly increases in off stoichiometric samples (after oxygen post-annealing) detectable by the Hall effect. The electrical activation energy has been determined as 0.17 eV (170 meV), and these complexes are responsible for forming an impurity band and hopping conductivity below 400 K.[32] It is suggested in this study that the non-equilibrium electrons in as-grown (close to stoichiometry) Ga_2O_3 thin films, generated during the excitation with an electron beam, are captured by V_{Ga}^{-}–V_O^{++} acceptor defect complexes. The thermal emission of these captured electrons is represented by activation energies extracted from EBIC and CL experiments. In other words, V_{Ga}^{-}–V_O^{++} acceptor complexes are detectable by electron beam excitation even in close to stoichiometric samples when electrical measurements are insensitive, probably due to their insufficient concentration. Moreover, based on the discussion given above, the nature of the native defects probed with EBIC and CL in both samples is alike. The difference in the activation energies is primarily due to the difference in their concentration, which is governed by the oxygen partial pressure during the growth process. The process of non-equilibrium electron detrapping in this work has an analogy with Mg-doped p-GaN, where the release of a non-equilibrium electron from deep acceptor levels is seen in the thermal activation of L.[65]

In summary, EBIC and CL techniques were employed to understand the temperature dependence of the diffusion length of

minority carriers and CL emission in p-type β-Ga_2O_3 with two different hole concentrations. Optical signatures of native acceptor defects (isolated V_{Ga} and V_{Ga}^{-}–V_O^{2+} complex) were identified in the CL spectrum. In addition, the activation energies for change of L with temperature ($\Delta E_{L,T}$) and thermal quenching of CL intensity (ΔE_{CL}) were experimentally obtained as 67 and 88 meV for sample A and 113 and 101 meV for sample B within the temperature range of 304–404 K. Comparable values of $\Delta E_{L,T}$ and ΔE_{CL} indicate a common origin for both processes, which is attributed to the thermal de-trapping of electrons from the V_{Ga}^{-}–V_O^{++} acceptor level. The current development in the characterization of p-type β-Ga_2O_3 could serve a pivotal role in realizing bipolar gallium oxide devices.

The research at UCF was supported, in part, by the NSF (Grant Nos. ECCS1802208 and ECCS2127916). The research at UCF and Tel Aviv University was supported partially by the US–Israel BSF (Award No. 2018010) and NATO (Award No. G5748). The work at UF was performed as part of the Interaction of Ionizing Radiation with Matter University Research Alliance (IIRM-URA), sponsored by the Department of the Defense, Defense Threat Reduction Agency (Award No. HDTRA1-20-2-0002), monitored by Jacob Calkins and by the NSF DMR (Grant No. 1856662) (J. H. Edgar). This work is a part of the "GALLIA" International Research Project, CNRS, France.

AUTHOR DECLARATIONS

Conflict of Interest

The authors have no conflicts to disclose.

DATA AVAILABILITY

The data that support the findings of this study are available from the corresponding author upon reasonable request.

REFERENCES

[1] S. I. Stepanov, V. I. Nikolaev, V. E. Bougrov, and A. E. Romanov, Rev. Adv. Mater. Sci. **44**, 63 (2016).
[2] M. Kim, J.-H. Seo, U. Singisetti, and Z. Ma, J. Mater. Chem. C **5**, 8338 (2017).
[3] S. J. Pearton, J. Yang, P. H. Cary, F. Ren, J. Kim, M. J. Tadjer, and M. A. Mastro, Appl. Phys. Rev. **5**, 011301 (2018).
[4] Progress in semiconductor *β*-Ga_2O_3," in *Ultra-Wide Bandgap Semiconductor Materials*, edited by M. Liao, B. Shen, and Z. Wang (Elsevier, 2019), pp. 263–345.
[5] M. J. Tadjer, J. L. Lyons, N. Nepal, J. A. Freitas, A. D. Koehler, and G. M. Foster, ECS J. Solid State Sci. Technol. **8**, Q3187 (2019).
[6] J. Zhang, J. Shi, D.-C. Qi, L. Chen, and K. H. L. Zhang, APL Mater. **8**, 020906 (2020).
[7] J. Y. Tsao, S. Chowdhury, M. A. Hollis, D. Jena, N. M. Johnson, K. A. Jones, R. J. Kaplar, S. Rajan, C. G. Van de Walle, E. Bellotti, C. L. Chua, R. Collazo, M. E. Coltrin, J. A. Cooper, K. R. Evans, S. Graham, T. A. Grotjohn, E. R. Heller, M. Higashiwaki, M. S. Islam, P. W. Juodawlkis, M. A. Khan, A. D. Koehler, J. H. Leach, U. K. Mishra, R. J. Nemanich, R. C. N. Pilawa-Podgurski, J. B. Shealy, Z. Sitar, M. J. Tadjer, A. F. Witulski, M. Wraback, and J. A. Simmons, Adv. Electron. Mater. **4**, 1600501 (2018).
[8] H. von Wenckstern, Adv. Electron. Mater. **3**, 1600350 (2017).
[9] M. Higashiwaki, K. Sasaki, H. Murakami, Y. Kumagai, A. Koukitu, A. Kuramata, T. Masui, and S. Yamakoshi, Semicond. Sci. Technol. **31**, 034001 (2016).
[10] K. Akito, K. Kimiyoshi, W. Shinya, Y. Yu, M. Takekazu, and Y. Shigenobu, Jpn. J. Appl. Phys. **55**, 1202A2 (2016).
[11] H. J. von Bardeleben and J. L. Cantin, J. Appl. Phys. **128**, 125702 (2020).
[12] E. B. Yakimov, A. Y. Polyakov, N. B. Smirnov, I. V. Shchemerov, P. S. Vergeles, E. E. Yakimov, A. V. Chernykh, M. Xian, F. Ren, and S. J. Pearton, J. Phys. D: Appl. Phys. **53**, 495108 (2020).
[13] A. K. Rajapitamahuni, L. R. Thoutam, P. Ranga, S. Krishnamoorthy, and B. Jalan, Appl. Phys. Lett. **118**, 072105 (2021).
[14] Z. Kabilova, C. Kurdak, and R. L. Peterson, Semicond. Sci. Technol. **34**, 03LT02 (2019).
[15] A. J. Green, K. D. Chabak, E. R. Heller, R. C. Fitch, M. Baldini, A. Fiedler, K. Irmscher, G. Wagner, Z. Galazka, S. E. Tetlak, A. Crespo, K. Leedy, and G. H. Jessen, IEEE Electron Device Lett. **37**, 902 (2016).
[16] M. H. Wong, K. Sasaki, A. Kuramata, S. Yamakoshi, and M. Higashiwaki, IEEE Electron Device Lett. **37**, 212 (2016).
[17] M. Higashiwaki, A. Kuramata, H. Murakami, and Y. Kumagai, J. Phys. D: Appl. Phys. **50**, 333002 (2017).
[18] G. Yang, S. Jang, F. Ren, S. J. Pearton, and J. Kim, ACS Appl. Mater. Interfaces **9**, 40471 (2017).
[19] K. Konishi, K. Goto, H. Murakami, Y. Kumagai, A. Kuramata, S. Yamakoshi, and M. Higashiwaki, Appl. Phys. Lett. **110**, 103506 (2017).
[20] S. Modak, L. Chernyak, S. Khodorov, I. Lubomirsky, J. Yang, F. Ren, and S. J. Pearton, ECS J. Solid State Sci. Technol. **8**, Q3050 (2019).
[21] S. Modak, J. Lee, L. Chernyak, J. Yang, F. Ren, S. J. Pearton, S. Khodorov, and I. Lubomirsky, AIP Adv. **9**, 015127 (2019).
[22] S. Modak, L. Chernyak, S. Khodorov, I. Lubomirsky, A. Ruzin, M. Xian, F. Ren, and S. J. Pearton, ECS J. Solid State Sci. Technol. **9**, 045018 (2020).
[23] S. Modak, L. Chernyak, A. Schulte, M. Xian, F. Ren, S. J. Pearton, I. Lubomirsky, A. Ruzin, S. S. Kosolobov, and V. P. Drachev, Appl. Phys. Lett. **118**, 202105 (2021).
[24] S. Modak, L. Chernyak, A. Schulte, M. Xian, F. Ren, S. J. Pearton, A. Ruzin, S. S. Kosolobov, and V. P. Drachev, AIP Adv. **11**, 125014 (2021).
[25] Y. Yan and S. H. Wei, Phys. Status Solidi B **245**, 641 (2008).
[26] H. Gao, S. Muralidharan, N. Pronin, M. R. Karim, S. M. White, T. Asel, G. Foster, S. Krishnamoorthy, S. Rajan, L. R. Cao, M. Higashiwaki, H. von Wenckstern, M. Grundmann, H. Zhao, D. C. Look, and L. J. Brillson, Appl. Phys. Lett. **112**, 242102 (2018).
[27] S. Marcinkevičius and J. S. Speck, Appl. Phys. Lett. **116**, 132101 (2020).
[28] M. D. McCluskey, J. Appl. Phys. **127**, 101101 (2020).
[29] Y. K. Frodason, K. M. Johansen, L. Vines, and J. B. Varley, J. Appl. Phys. **127**, 075701 (2020).
[30] T. D. Gustafson, J. Jesenovec, C. A. Lenyk, N. C. Giles, J. S. McCloy, M. D. McCluskey, and L. E. Halliburton, J. Appl. Phys. **129**, 155701 (2021).
[31] E. Chikoidze, A. Fellous, A. Perez-Tomas, G. Sauthier, T. Tchelidze, C. Ton-That, T. T. Huynh, M. Phillips, S. Russell, M. Jennings, B. Berini, F. Jomard, and Y. Dumont, Mater. Today Phys. **3**, 118 (2017).
[32] E. Chikoidze, C. Sartel, H. Mohamed, I. Madaci, T. Tchelidze, M. Modreanu, P. Vales-Castro, C. Rubio, C. Arnold, V. Sallet, Y. Dumont, and A. Perez-Tomas, J. Mater. Chem. C **7**, 10231 (2019).
[33] X. Wang, T. Liu, Y. Lu, Q. Li, R. Guo, X. Jiao, and X. Xu, J. Phys. Chem. Solids **132**, 104 (2019).
[34] C. A. Dimitriadis, J. Phys. D: Appl. Phys. **14**, 2269 (1981).
[35] L. Chernyak, A. Osinsky, H. Temkin, J. W. Yang, Q. Chen, and M. Asif Khan, Appl. Phys. Lett. **69**, 2531 (1996).
[36] V. K. S. Ong, O. Kurniawan, G. Moldovan, and C. J. Humphreys, J. Appl. Phys. **100**, 114501 (2006).
[37] N. Ma, N. Tanen, A. Verma, Z. Guo, T. Luo, H. Xing, and D. Jena, Appl. Phys. Lett. **109**, 212101 (2016).
[38] A. Y. Polyakov, I.-H. Lee, N. B. Smirnov, E. B. Yakimov, I. V. Shchemerov, A. V. Chernykh, A. I. Kochkova, A. A. Vasilev, F. Ren, P. H. Carey, and S. J. Pearton, Appl. Phys. Lett. **115**, 032101 (2019).
[39] A. Y. Polyakov, N. B. Smirnov, I. V. Shchemerov, E. B. Yakimov, S. J. Pearton, C. Fares, J. Yang, F. Ren, J. Kim, P. B. Lagov, V. S. Stolbunov, and A. Kochkova, Appl. Phys. Lett. **113**, 092102 (2018).
[40] E. B. Yakimov, A. Y. Polyakov, N. B. Smirnov, I. V. Shchemerov, J. Yang, F. Ren, G. Yang, J. Kim, and S. J. Pearton, J. Appl. Phys. **123**, 185704 (2018).

[41] J. Lee, E. Flitsiyan, L. Chernyak, J. Yang, F. Ren, S. J. Pearton, B. Meyler, and Y. J. Salzman, Appl. Phys. Lett. **112**, 082104 (2018).
[42] M. M. R. Adnan, D. Verma, Z. Xia, N. K. Kalarickal, S. Rajan, and R. C. Myers, Phys. Rev. Appl. **16**, 034011 (2021).
[43] O. Lopatiuk-Tirpak, L. Chernyak, F. X. Xiu, J. L. Liu, S. Jang, F. Ren, S. J. Pearton, K. Gartsman, Y. Feldman, A. Osinsky, and P. Chow, J. Appl. Phys. **100**, 086101 (2006).
[44] M. Eckstein and H.-U. Habermeier, J. Phys. IV **01**, C6-23 (1991).
[45] S. Yamaoka and M. Nakayama, Phys. Status Solidi C **13**, 93 (2016).
[46] P. Deák, Q. Duy Ho, F. Seemann, B. Aradi, M. Lorke, and T. Frauenheim, Phys. Rev. B **95**, 075208 (2017).
[47] Q. D. Ho, T. Frauenheim, and P. Deák, Phys. Rev. B **97**, 115163 (2018).
[48] J. Lapp, D. Thapa, J. Huso, A. Canul, M. McCluskey, and L. Bergman, Bull. Am. Phys. Soc. **65**, 245 (2020).
[49] T. Onuma, S. Fujioka, T. Yamaguchi, M. Higashiwaki, K. Sasaki, T. Masui, and T. Honda, Appl. Phys. Lett. **103**, 041910 (2013).
[50] B. E. Kananen, N. C. Giles, L. E. Halliburton, G. K. Foundos, K. B. Chang, and K. T. Stevens, J. Appl. Phys. **122**, 215703 (2017).
[51] A. Y. Polyakov, I.-H. Lee, N. B. Smirnov, A. V. Govorkov, E. A. Kozhukhova, N. G. Kolin, A. V. Korulin, V. M. Boiko, and S. J. Pearton, J. Appl. Phys. **109**, 123703 (2011).
[52] E. B. Yakimov, A. Y. Polyakov, I. V. Shchemerov, N. B. Smirnov, A. A. Vasilev, P. S. Vergeles, E. E. Yakimov, A. V. Chernykh, F. Ren, and S. J. Pearton, Appl. Phys. Lett. **118**, 202106 (2021).
[53] L. Binet and D. Gourier, J. Phys. Chem. Solids **59**, 1241 (1998).
[54] K. Shimamura, E. G. Víllora, T. Ujiie, and K. Aoki, Appl. Phys. Lett. **92**, 201914 (2008).
[55] S. Yamaoka, Y. Furukawa, and M. Nakayama, Phys. Rev. B **95**, 094304 (2017).
[56] T. T. Huynh, L. L. C. Lem, A. Kuramata, M. R. Phillips, and C. Ton-That, Phys. Rev. Mater. **2**, 105203 (2018).
[57] T. Onuma, Y. Nakata, K. Sasaki, T. Masui, T. Yamaguchi, T. Honda, A. Kuramata, S. Yamakoshi, and M. Higashiwaki, J. Appl. Phys. **124**, 075103 (2018).
[58] Y. Wang, P. T. Dickens, J. B. Varley, X. Ni, E. Lotubai, S. Sprawls, F. Liu, V. Lordi, S. Krishnamoorthy, S. Blair, K. G. Lynn, M. Scarpulla, and B. Sensale-Rodriguez, Sci. Rep. **8**, 18075 (2018).
[59] V. Vasyltsiv, A. Luchechko, L. Kostyk, and B. Pavlyk, in *2019 XIth International Scientific and Practical Conference on Electronics and Information Technologies (ELIT)* (IEEE, 2019).
[60] E. Nogales, J. A. García, B. Méndez, J. Piqueras, K. Lorenz, and E. Alves, J. Phys. D: Appl. Phys. **41**, 065406 (2008).
[61] E. G. Víllora, M. Yamaga, T. Inoue, S. Yabasi, Y. Masui, T. Sugawara, and T. Fukuda, Jpn. J. Appl. Phys. **41**, L622 (2002).
[62] X. T. Zhou, F. Heigl, J. Y. P. Ko, M. W. Murphy, J. G. Zhou, T. Regier, R. I. R. Blyth, and T. K. Sham, Phys. Rev. B **75**, 125303 (2007).
[63] G. Pozina, M. Forsberg, M. A. Kaliteevski, and C. Hemmingsson, Sci. Rep. **7**, 42132 (2017).
[64] Y. Nie, S. Jiao, S. Li, H. Lu, S. Liu, S. Yang, D. Wang, S. Gao, J. Wang, and Y. Li, J. Alloys Compd. **900**, 163431 (2021).
[65] L. Chernyak, A. Osinsky, V. Fuflyigin, and E. F. Schubert, Appl. Phys. Lett. **77**, 875 (2000).